Iran. J. Biotechnol. January 2023;21(1): e 3315 DOI: 10.30498/ijb.2022.334455.3315

Research Article

Phytate-Induced Dose-Response Auto-Activation of Enzyme in Commercial Recombinant Phytase From *Escherichia coli*

Elmira Naghdi[1], Zahra Moosavi-Nejad[1*],Bahman Gholamhossein Goudarzi[2,3], Mohammad Reza Soudi[4]

[1]Department of Biotechnology, Faculty of Biological Sciences, Alzahra University, Tehran, Iran
[2]Akam Faravardehaye Bahman Arad, Kamalshahr, Karaj, Iran
[3]Razi Vaccine and Serum Research Institute, Karaj, Iran
[4]Department of Microbiology, Faculty of Biological Sciences, Alzahra University, Tehran, Iran

[*]*Corresponding author*: Zahra Moosavi-Nejad, Department of Biotechnology, Faculty of Biological Sciences, Alzahra University, Tehran, Iran. Tel:+98-2185692952, Fax:+98-2188035187, E-mail: z.moosavinejad@alzahra.ac.ir

Received: 2022/03/16; **Accepted:** 2022/11/07

Background: Microbial phytase is one of the most widely used enzymes in food industries like cattle, poultry, and aquaculture food. Therefore, understanding the kinetic properties of the enzyme is very important to evaluate and predict its behavior in the digestive system of livestock. Working on phytase is one of the most challenging experiments because of some problems, including free inorganic phosphate (FIP) impurity in phytate (substrate) and interference reaction of the reagent with both phosphates (product and phytate impurity).

Objective: In the present study, FIP impurity of phytate was removed, and then it was shown that the substrate (phytate) has a dual role in enzyme kinetics: substrate and activator.

Material and Methods: phytate impurity was decreased by two-step recrystallization prior to the enzyme assay. The impurity removal was estimated by the ISO30024:2009 method and confirmed by Fourier-transform infrared (FTIR) spectroscopy. The kinetic behavior of phytase activity was evaluated using the purified phytate as substrate by non-Michaelis-Menten analysis, including Eadie-Hofstee, Clearance, and Hill plots. The possibility of an allosteric site on phytase was assessed by molecular docking.

Results: The results showed a 97.2% decrease in FIP due to recrystallization. The phytase saturation curve had a sigmoidal appearance, and Lineweaver-Burk plot with a negative y-intercept indicated the positive homotropic effect of the substrate on the enzyme activity. A right-side concavity of Eadie-Hofstee plot confirmed it. Hill coefficient was calculated to be 2.26. Molecular docking also showed that *Escherichia coli* phytase molecule has another binding site for phytate very close to the active site, called “allosteric site”.

Conclusions: The observations strongly propose the existence of an intrinsic molecular mechanism in *Escherichia coli* phytase molecules to be promoted for more activity by its substrate, phytate (positive homotropic allosteric effect). *In silico* analysis showed that phytate binding to the allosteric site caused new substrate-mediated inter-domain interactions, which seems to lead to a more active conformation of phytase. Our results provide a strong basis for animal feed development strategies, especially in the case of poultry food and supplements, regarding a short food passage time in their gastrointestinal tract and variable concentration of phytate along with it. Additionally, the results strengthen our understanding of phytase auto-activation as well as allosteric regulation of monomeric proteins in general.

Keywords: Auto-activation, *E. coli* phytase, Non-Michaelis kinetics, Phytate, Recrystallization

1. Background

Phosphate is one of the essential nutritional demands among animals. Existanse of the mineral form of phosphate in the feed leads to high costs and environmental problems (1). Animal diets are usually rich in phytate (*myo*-inositol hexakisphosphate). Phytate is a storage form of phosphate in plant seeds as the main component of animal food. Six phosphate groups are attached to a *myo*-inositol molecule in the phytate structure. Monogastric animals such as birds, fishes, or pigs cannot hydrolyze phytate to use its phosphates. Today, an enzyme superfamily called phytases (*myo*-inositol hexakisphosphate phosphohydrolase, EC 3.1.3.x (x = 8, 26 or 72)) is added to animals' diets to solve the problem. The enzyme can release phosphate from phytate, in addition to providing phosphate, reducing the chelating effects of phytate (2). Hence, today, phytase is a thriving enzyme in the livestock, poultry, and aquaculture industries.

Plants, bacteria, molds, yeasts, and animals can produce phytase. However, microorganisms are the most active living organism in producing phytases (3). Phytases are divided into four classes based on their biochemical properties and conserved sequences: histidine acid phosphatases, cysteine phosphatases, β-propeller phytases, and purple acid phosphatases. Phytases originating from *Aspergillus niger*, *Escherichia coli*, and *Peniophora lycii* belong to the histidine acid phosphatase family and have been commercialized (4). Phytase from *E. coli* is widely used in the animal's food industry. This enzyme has two structural domains called α and α/β domains, and its active site is in the form of a relatively large cavity between the two domains (5). Studies on *E. coli* phytase have shown that this enzyme has a high specificity for sodium phytate (6) and has the greatest specific activity among different classes of phytase (2).

Studies have shown that the binding of phytate to the active site of *E. coli* phytase leads to conformational changes in the enzyme's structure (5). However, the possibility of a phytate binding to a site other than the active site was not yet been investigated. If the binding of the second phytate led to any change in phytase activity, the phenomenon would be an allosteric regulation by its substrate, known as "homotropic effect" (7).

Allosteric regulation is widely used in various industries. For example, in the therapeutic field, identifying allosteric sites is the first step in discovering and designing drugs whose action enhances the enzyme's function (8). The allosteric behavior of some enzymes is also used in producing highly sensitive biosensors (9). In addition, in today's food industry, identifying sweet taste receptors with positive allosteric modulation provides the conditions to replace sweeteners with compounds that stimulate the taste sensation very well (10). Allosteric regulation is so valuable that sometimes attempts are made to create this property in the desired enzyme by adding a new domain (11).

2. Objectives

In this study, we have recrystallized commercial sodium phytate to reduce its FIP impurity. Then, we investigated the role of phytate in *E. coli* phytase activity, not only as a substrate but also as an allosteric activator. Moreover, the existence of an allosteric site for phytate has been predicted using the molecular docking method, and we have proposed a probable mechanism for allosteric behavior in *E. coli* phytase via new phytate-mediated inter-domain interactions. We have also discussed the importance of our findings in the animal food industry.

3. Materials and Methods

Commercial phytase (Smizyme TS G5, Beijing smile) was donated by Golbid Company (Tehran, Iran). This enzyme is a pure cloned 6-phytase derived from *E. coli*, expressed in *Pichia pastoris*. Sodium phytate (P8810), ammonium heptamolybdate, and ammonium metavanadate were from Sigma-Aldrich. All other chemicals used in this study were of analytical grade.

3.1. Sodium Phytate Recrystallization

FIP impurity in phytate was removed by the recrystallization technique (12). FIP content (μmol of free inorganic phosphate per mg of phytate) was measured before and after recrystallization using a colorimetric method with heptamolybdate/vanadate reagent (See phytase assay).

3.2. Fourier Transform Infrared (FTIR) Spectroscopy

Phytate chemical structure was examined in the transmission mode using a Bruker FTIR spectrometer (Tensor 27) by KBr pellet technique in the wavenumber range of 400 to 4000 cm^{-1} and resolution 0.1%T. The powdered phytate before and after recrystallization was used to make pellets. All spectra were baseline

corrected.

3.3. Phytase Assay

The International Standard for Measuring Phytase Activity (ISO 30024:2009) was used to measure phytase activity based on measuring the product. According to this method, FIP reacts with ammonium molybdate under acidic conditions in the presence of vanadium to form yellowish vanadomolybdophosphoric acid. The intensity of the yellow color corresponds to the concentration of FIP. Phytase activity was measured by mixing 360 µL of 0.25 M acetate buffer pH 5.5 with 0.01% mass fraction polysorbate 20 and 40µL of phytase solution. The enzymatic reactions were initiated by adding 800 µL of 7.5 mM sodium phytate to meet the desired concentration. The solution was incubated for exactly 30 min at 37 °C. Then 800 µL of freshly-prepared stop reagent (ammonium heptamolybdate 10% (w/v): ammonium vanadate 0.235% (w/v): nitric acid 21.66% (v/v) with 1:1:2 ratio) was added. The reaction mixture was incubated at room temperature for 10 minutes and centrifuged at 11000 ×g for 3 min. FIP concentration was determined based on the absorbance of the supernatant at 415 nm using KH_2PO_4 standard curve. Initial velocity (V) was considered as the change of FIP concentration after 30 min incubation of the enzyme-substrate mixture.

3.4. Steady-State Kinetic Data

Initial measurements were carried out in assay conditions as mentioned in "phytase assay" at various initial phytate concentrations (0-1.25 mM), and the experimental data were used for plotting the saturation curve of phytase (Michaelis-Menten Plot) using least-squares nonlinear regression. The calculated phytate binding in Michaelis-Menten plot was best described by Hill-Langmuir equation (equation 1):

$$v = \frac{V_{max} \times [S]^{n}}{[S]_{50}^{n} + [S]^{n}} \qquad (1)$$

where v and V_{max} are the calculated and apparent maximum activity of experimental data, respectively, $[S]_{50}$ is the concentration of phytate at $V_{max}/2$, [S] is phytate concentration, and n is Hill coefficient (resulted from Hill plot). The "n" was assumed to be equal to unit for hypothetical Michaelis kinetics and 2.27 for theoretical non-Michaelis kinetics.

Moreover, the kinetic data of the initial reaction velocities were plotted according to Lineweaver-Burk (1/v *vs* 1/[S]), Eadie-Hofstee (v *vs* v/[S]), Clearance (v/[S] *vs* log[S]) and Hill (log(v/(V_{max}-v)) *vs* log [S]) and fitted. Lineweaver-Burk and Eadie-Hofstee plots provide graphical information about enzyme behavior rather than kinetic parameters. The slope of Hill plot was used as Hill coefficient (n).

3.5. Molecular Docking Prediction

Auto Dock Vina software predicted the second phytate binding site on phytase. The protein file 1DKQ was downloaded from the Protein Data Bank (PDB; http://www.rcsb.org/pdb/). Further analyzes were performed using Auto Dock Tools (v.1.5.6), Discovery Studio (v.21.1.0.20298), Ligplot^{+} (v.1.4.5), and chimera (v.1.15) software.

3.6. Statistical Analysis

The statistical analysis and data fitting were performed using the software package "MS Excel 2016".

4. Results

4.1. Sodium Phytate Recrystallization

In order to obtain a proper and confident saturation curve of phytase, a two-stage phytate crystallization method was initially performed to minimize the FIP impurity. The content of FIP in sodium phytate was measured before and after the recrystallization of sodium phytate by the colorimetric method. The results showed a 97.2% decrease in FIP due to recrystallization **(Fig. 1A)**. The FTIR spectrum was recorded to ensure the integrity of the phytate chemical structure and to confirm the reducing FIP impurity by the recrystallization process **(Fig. 1B)**.

4.2. Determination of Kinetic Parameters

E. coli phytase saturation curve was plotted against different concentrations of sodium phytate **(Fig. 2A)**. The graphical appearance of the saturation curve was not hyperbolic but sigmoid. The appearance of Lineweaver-Burk's plot was unusual, and the y-intercept of the resulting line was negative **(Fig. 2B)**. In order to find out the reason for these observations and to assess whether the kinetic behavior of the enzyme follows the Michaelis Menten model or not, the Eddie-Hofsti curve was plotted **(Fig. 2C)**.

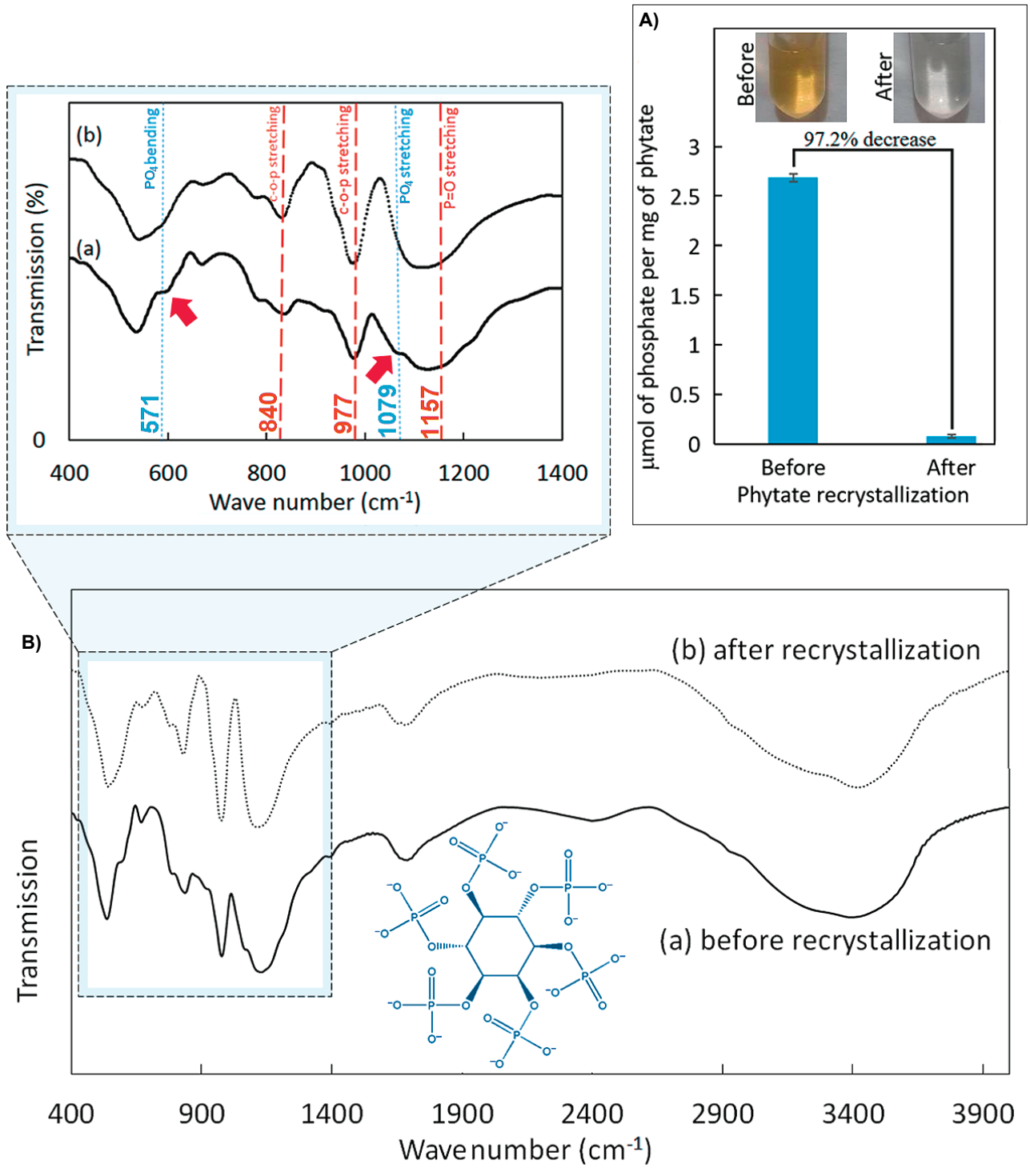

Figure 1. Improvement of sodium phytate purity by recrystallization. A) Quantitative colorimetric test for measuring free Inorganic phosphate (FIP) content before and after recrystallization of commercial sodium phytate (FIP concentration is proportional to the intensity of the yellow color). **B)** Fourier transform infrared (FTIR) spectra of sodium phytate before **(a)** and after **(b)** recrystallization (inset: chemical structure of phytate). The orange and blue dashed lines are related to phytate and FIP, respectively.

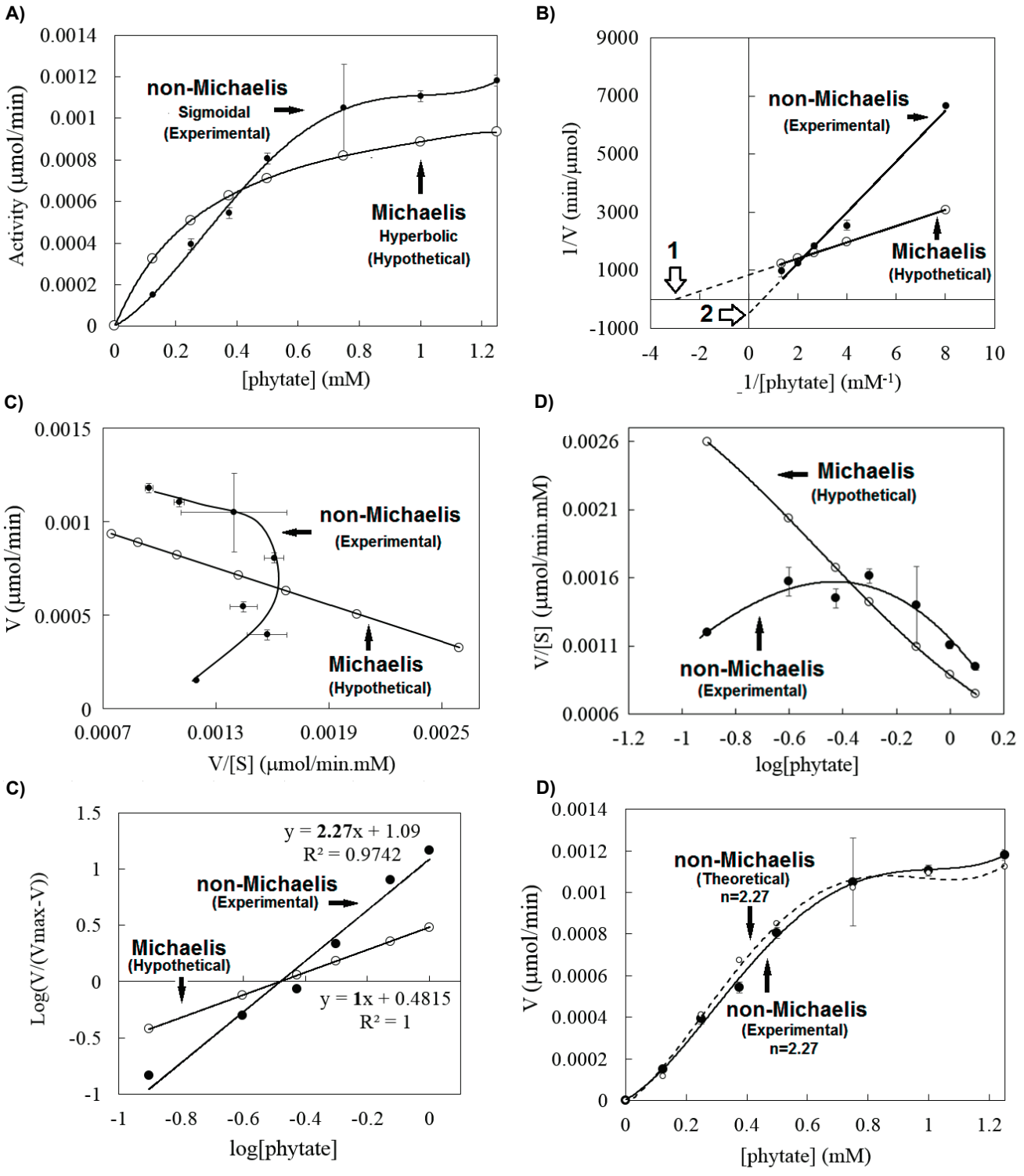

Enzyme	$[S]_{50}$ (mM)	V_{max} (µmol.min^{-1})	n
E.coli phytase	0.33	0.0012	2.27

Figure 2. Kinetic analysis of phytase experimental data (•) compared to the hypothetical Michaelis model (°). **A)** Saturation curve, and **B)** Lineweaver-Burk. **C)** Eadie-Hofstee. **D)** Clearance. **E)** Hill plots. **F)** Experimental saturation curve (black line) compared to the best-fitting Hill-Langmuir equation curve (dash line). The table at the bottom: kinetics parameter of non-Michaelis behavior of the phytase.

A convexity was observed to the right side of the Eadie-Hofstee plot. The clearance plot was also Convex **(Fig. 2D)**. Hill plot was drawn and showed a line with a slope of 2.27 **(Fig. 2E)**.

4.3. Molecular Docking Investigation

Molecular docking was performed *in silico* to investigate the existence of the second binding site of the substrate between the phytase-phytate complex (1DKQ) and the substrate **(Fig. 3A)**. The amino acids around the first substrate-binding site (active site) and the second substrate-binding site (allosteric site), as well as their hydrogen and hydrophobic interactions, were analyzed using Ligplot^{+} **(Fig. 3A)**. The allosteric site is located between the two structural domains of phytase **(Fig. 3B)**. Contact maps of the amino acids around the active and allosteric sites are depicted in the separate domains **(Fig. 3C)**. The binding of the second substrate added six new hydrogen bonds and four new hydrophobic interactions between the two domains through the second phytate **(Fig. 3D)**, introducing 150 kJ.moL^{-1} and 4 kJ.moL^{-1} interdomain binding energy, respectively **(Fig. 3E)**. The position of the amino acids involved in interactions with phytates at active and allosteric sites by structural domains was represented using chimera software **(Fig. 4A)**. The binding affinity of the first and second substrate molecules was estimated to be 3.15×10^{5} and 4.15×10^{4} M^{-1}, respectively.

5. Discussion

To determine beneficial, effective, safe, or hazardous dosages of foods, nutrients, drugs, or pollutants, "dose-response" studies and their related models are significant and often affect public policy. "Dose-response" relationships can describe how a group of molecules or organisms respond to various levels of exposure. The saturation curve (Michaelis-Menten) of enzymes by their substrate(s) is a famous example of dose-response models used in the food and pharmaceutical industries as well as biosensor technology (9, 10, 13). In this study, dose-response regulation of *E. coli* phytase activity has been studied.

Microbial phytases cause the gradual release of FIP from phytate (1). Since FIP is not a chromophore (14), indirect colorimetric methods are often used to measure its concentration (15, 16). Assaying phytase using commercial phytate with high FIP impurity is not acceptable, which results in non-reproducible activity measurements. Moreover, many researchers have pointed out the inhibitory effect of FIP on phytase activity (6, 17). furthermore, based on the International Standard, phytate's inorganic phosphorus content should be ≤0.1 % mass fraction (ISO 30024:2009). This protocol suggests phytate, Sigma P0109, from rice, for use as a phytase substrate due to its low FIP content, but this product is not commercially available now. Sigma P8810, from rice, is an available alternative with relatively more FIP impurity. Fortunately, it has recently been shown that P8810 can be more purified via the recrystallization method confirmed by HPLC (12). So, we have recrystallized sodium phytate before measuring enzyme activity. As the main evidence for successful reduction of FIP, the colorimetric method showed 97.2% of FIP purification **(Fig. 1A).** The FTIR result also confirmed the purification: the two peaks at 571 and 1079 cm^{-1} (blue dashed lines) were removed after recrystallization. These peaks belong to the bending and stretching forces of FIP impurity (18, 19). Meanwhile, the three characteristic peaks of sodium phytate at the wavenumber of 840 cm^{-1} (C-O-P stretching), 977cm^{-1} (C-O-P stretching), and 1157 cm^{-1} (P=O stretching) (20) were also observed after recrystallization **(Fig. 1B)**. Therefore, the recrystallization decreased large amounts of FIP impurity in sodium phytate, making it a reliable substrate for studying phytase activity.

An enzyme's most well-known and applicable characteristic is K_m (Michaelis constant), a measure of an enzyme affinity for a given substrate. The estimation of K_m using Lineweaver-Burk plot is based on the assumption that the enzyme's affinity to the substrate is not dependent on the substrate concentration (hyperbolic saturation curve). Although it is easy to check this assumption, researchers usually do not check it. In the case of phytase, there are numerous reports on its kinetic parameters, but most of them do not present the enzyme saturation curve (Michaelis-Menten plot), which makes them difficult to be checked for the above assumption. In these studies, the enzyme is mainly assumed to follow "Michaelis behavior" without evaluating the correctness of the assumption (6, 21, 22). On the other hand, there is a report on non-Michaelis behavior of some phytases (without displaying the data) (17).

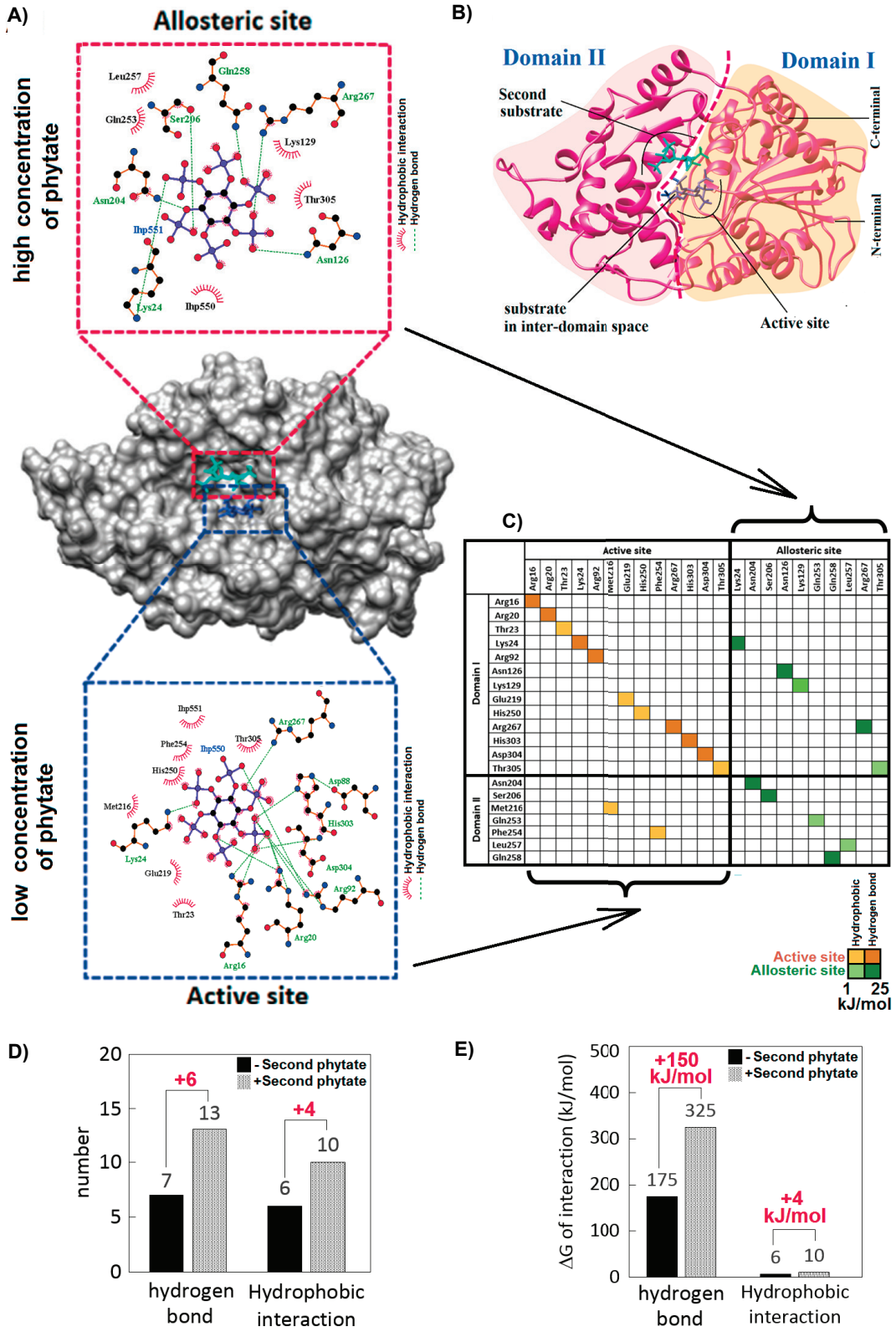

Figure 3. Enzyme-substrate interactions analysis. A) Ligplot+ image of interactions around the active site (down) and the allosteric site (up) of *E. coli* phytase with two phytate molecules. **B)** The binding position of the first and second substrates between the enzyme structural domains. **C)** Contact map for active site and allosteric site. **D)** The change of interdomain interactions through the second phytate binding. **E)** The change in energy of the interdomain interactions through the second phytate binding

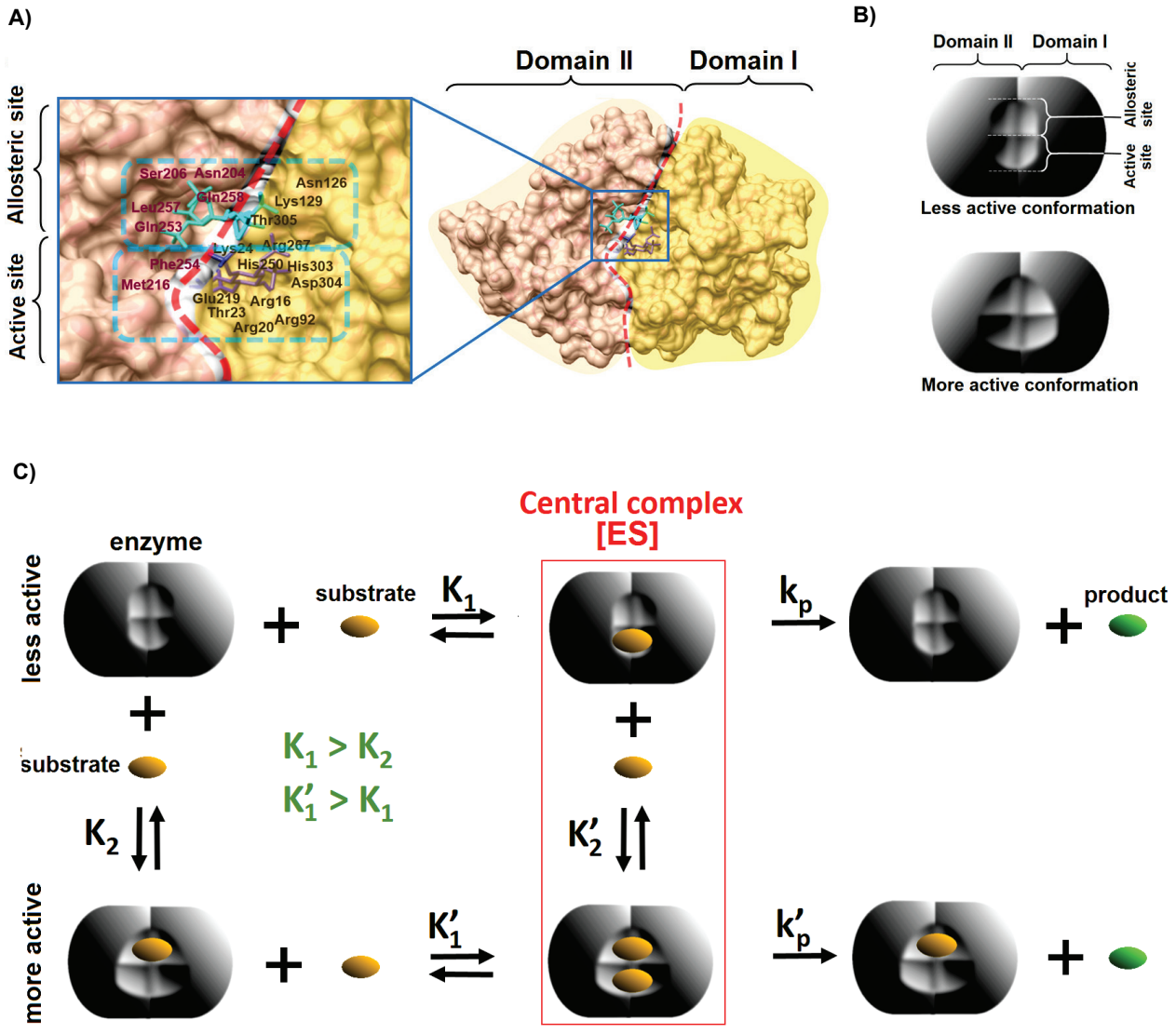

Figure 4. **Conformational changes in the phytase through the second substrate binding. A)** The position of the amino acids involved in interactions with phytates at active and allosteric sites between two structural domains of *E. coli* phytase. **B)** Schematic representation of two different conformations of the enzyme. **C)** A model for the allosteric activation of *E. coli* phytase by its substrate (auto-activation).

Because of the importance of accurate determination of phytase kinetic behavior, in the present study, the exact kinetic behavior of *E. coli* phytase has been determined using a reliable substrate for the first time. The results showed that the phytase's saturation curve is not hyperbolic and has a sigmoidal appearance **(Fig. 2A)**. Furthermore, Lineweaver-Burk's plot has a negative *y*-intercept **(Fig. 2B)**, with an incorrect "negative" maximum velocity. These data show that the kinetic behavior of *E. coli* phytase does not follow the Michaelis-Menten model. Non-Michaelis-Menten behavior has previously been observed in *M. thermophila* and *A. nidulans* phytases (17). In Eadie-Hofstee plot, the curve convexity on the right side **(Fig. 2C)** graphically confirms a kind of non-Michaelis behavior called "positive homotropism" (7). Positive homotropism is a kind of allosteric regulation in which the activating regulator is the same substate, also

known as "auto-activation". Similarly, the upward convexity of Clearance plot confirmed the auto-activation behavior **(Fig. 2D)**. In order to quantify the auto-activation, Hill diagram was plotted for *E. coli* phytase, and Hill coefficient (n) was calculated to be 2.27 **(Fig. 2E)**. Hill coefficient is a tool to indicate and evaluate the amount of homotropic effect. In enzymes with Michaelis behavior, n=1. In enzymes with non-Michaelis behavior, n>1 and n<1 in the case of positive and negative homotropic effects, respectively. That means the substrate can up-regulate (n>1) or down-regulate (n<1) the activity of its enzyme (23). Therefore, Hill coefficient confirms that the substrate (phytate) has a dual role in enzyme kinetics: substrate and activator. Most allosteric enzymes are structurally multimeric, however, it has been a long time since the structural basis of allosterism in monomeric enzymes has been explained (24). Therefore, it is not surprising that *E. coli* phytase, as a monomeric enzyme (21), exhibits an allosteric behavior.

In the monomeric structure of *E. coli* phytase, the allosteric site was predicted to be very close to the active site **(Fig. 3A)**. That means while the first substrate occupied the active site (at low concentrations of phytate in the saturation curve in **Fig. 2A**), the second substrate could bind to the allosteric site at higher substrate concentrations. Generally, in the sigmoidal saturation curve of an enzyme, the substrate just occupies the active site at low concentrations of substrate because of the high affinity of the active site. But the possibility of substrate binding to the allosteric site (with lower affinity) increases by increasing the substrate concentration. This is correct in all positive allosterism. In the article related to PDB:1dkq, phytase is in solid state (not solution) with the highest compactness. Then the phytase crystal was soaked in a 3mM concentration of sodium phytate solution (5). Because the molar ratio of substrate to the enzyme is much lower than the actual condition of the enzyme assay solution, the substrate can only bind to the active site of phytase crystallized molecules. Moreover, when an enzyme molecule is in the crystal state, it has the highest structural compactness and the least structural flexibility. Therefore, the enzyme flexibility is not enough for the binding of the second substrate molecule to the allosteric site.

The binding of a second substrate in the allosteric position strengthened the relationship between the two domains through non-covalent interactions **(Fig. 3C and D)** and their related energies **(Fig. 3E)**. These changes induce a new conformation of the enzyme molecule **(Fig. 4B)**, which has more enzymatic activity according the experimental data of this study (logarithmic phase of sigmoidal saturation curve in **Fig. 2A** and **Fig. 5A**). So, the binding affinity of the substrate to the active site (3.15×10^5 M^{-1}) is 10-fold more than the affinity of the substrate to the allosteric site (4.15×10^4 M^{-1}). So it can be concluded that when the substrate concentration is low, the substrate binds to the enzyme's active sites (beginning part of the saturation curve), but an increase in substrate concentration causes the binding of the second substrate to the allosteric site. As a result, the saturation curve leaves the hyperbolic trend and becomes sigmoidal. Therefore, we suggest that *E. coli* phytase has two "less active" and "more active" conformations based on experimental and computational data. At low substrate concentrations, the molecular population of the "less active" conformation is predominant, and at high substrate concentrations, the "more active" conformation becomes predominant. Binding of the substrate molecule to the allosteric site with an affinity (K_2) less than the affinity for the active site (K_1) leads to the conversion of "less active" conformation to the "more active" conformations (with more affinity to the substrate: K'_1). Consequently, the concentration of the central complex increases and leads to more formation of the product **(Fig. 4C)**. In other words, the substrate molecule (phytate) plays a dual role in the enzyme's function: at low concentrations, it plays the role of substrate, and at high concentrations, it also plays the role of an activator.

The amount of phytate in animal food and different parts of the chicken digestive tract has been estimated (25). Due to digestion, phytate concentration is reduced from crop to gizzard **(Fig. 5B)**, which are the most important parts of phytase activity. by comparing the concentration range with the range of this study, it is clear that the described self-regulatory mechanism occurs in the chicken digestive tract.

6. Conclusion

The present study has emphasized the characterization of the allosteric behavior of commercial phytase from *E. coli* as a monomeric enzyme. Hill fitting of experimental data showed at least two binding sites for the substrate (phytate) on the phytase molecule, but only one is an active site, and the other is an allosteric

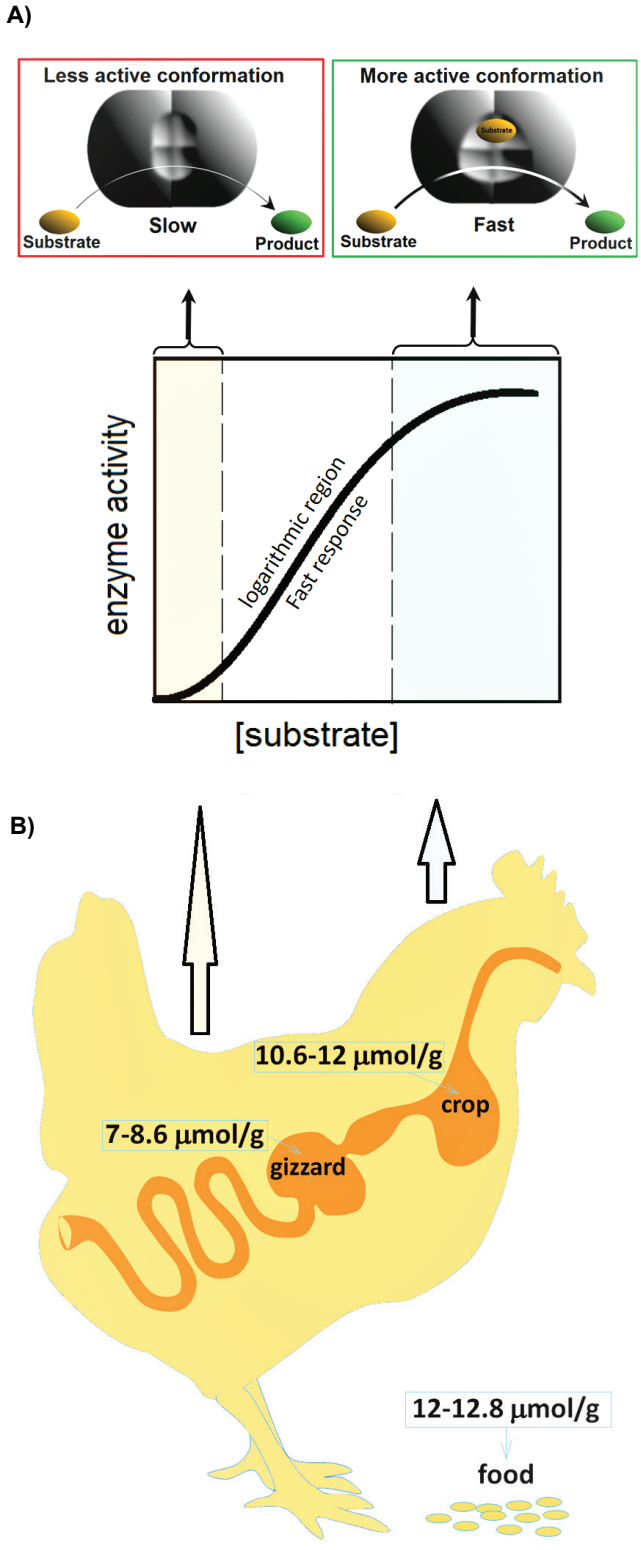

Figure 5. Accordance of decreasing phytate concentration in the chicken digestive tract with dose-dependency of *E. coli* phytase activity. A) Dose-dependent conformational and activity change of *E. coli* phytase molecule. **B)** Phytate content of food in the chicken digestive tract.

site. For the phytase, the allosteric behavior originates from the conformational relationship between the active site and the non-catalytic allosteric site both for the substrate, phytate, a phenomenon never reported before for phytase. With taking into account this model, the existence of two different conformational states of the enzyme was postulated: one in the low concentrations of the substrate, which is less active conformation, and the second in the higher concentrations of substrate, when the allosteric site is occupied by the substrate and acts as an allosteric activator. This plausible model has been supported by *in silico* study, which shows that binding of the second substrate molecule triggers new additional inter-domain interactions, which results in an allosteric characteristic to the phytase molecule. The results provide a strong basis for animal feed development strategies, especially in the case of poultry food and supplements, regarding a short feed passage time in their gastrointestinal tract and variable concentrations of phytate along with it. Additionally, the results strengthen our understanding of phytase kinetics and structure-function relationships. Furthermore, the results improve the current knowledge of allosteric regulation of monomeric proteins in general.

Acknowledgments

Alzahra University is acknowledged for providing funds and facilities to carry out this research. We thank the Akam Faravardehaye Bahman Arad Company for their valuable scientific advice and financial support for this research. We would also like to express our gratitude and appreciation to Golbid company for donating commercial phytase.

References

1. Gessler NN, Serdyuk EG, Isakova EP, Deryabina YI. Phytases and the Prospects for Their Application (Review). *Appl Biochem Microbiol*. 2018;**54**(4):352-360. doi:10.1134/s0003683818040087
2. Wodzinski RJ, Ullah A. Phytase. *Adv Appl Microbiol*. 1996;**42**(42). doi:10.1016/s0065-2164(08)70375-7
3. Dvořáková J. Phytase: Sources, Preparation and Exploitation. *Folia Microbiologica*. 1998;**43**(4):323-338. doi:10.1007/bf02818571
4. Hill JE, Richardson AE, Turner B. Isolation and assessment of microorganisms that utilize phytate. Inositol phosphates: Linking agriculture and the environment. 2007:61-77. doi: 10.1079/9781845931520.0061
5. Lim D, Golovan S, Forsberg CW, Jia Z. Crystal structures of Escherichia coli phytase and its complex with phytate. *Nat Struct Biol*. 2000;**7**(2):108-113. doi:10.2210/pdb1dkq/pdb
6. Greiner R, Konietzny U, Jany KD. Purification and characterization of two phytases from Escherichia coli. *Arch*

Biochem Biophys. 1993;**303**(1):107-113. doi:10.1006/abbi.1993.1261
7. Atkins WM. Non-Michaelis-Menten kinetics in cytochrome P450-catalyzed reactions. *Annu Rev Pharmacol Toxicol*. 2005;**45**:291-310. doi:10.1146/annurev.pharmtox.45.120403.100004
8. Rocheville M, Garland SL. An industrial perspective on positive allosteric modulation as a means to discover safe and selective drugs. *Drug Discov Today Technol*. 2010;**7**(1):e87-e94. doi:10. 1016/j.ddtec.2010.06.004
9. Guerrieri A, Ciriello R, Bianco G, De Gennaro F, Frascaro S. Allosteric Enzyme-Based Biosensors-Kinetic Behaviours of Immobilised L-Lysine-alpha-Oxidase from Trichoderma viride: pH Influence and Allosteric Properties. *Biosensors* (*Basel*). 2020;**10**(10). doi:10.3390/bios10100145
10. Servant G, Tachdjian C, Li X, Karanewsky DS. The sweet taste of true synergy: positive allosteric modulation of the human sweet taste receptor. *Trends Pharmacol Sci*. 2011;**32**(11):631-636. doi:10.1016/j.tips.2011.06.007
11. Guntas G, Ostermeier M. Creation of an allosteric enzyme by domain insertion. *J Mol Biol*. 2004;**336**(1):263-273. doi:10.1016/j.jmb.2003.12.016
12. Madsen CK, Brearley CA, Brinch-Pedersen H. Lab-scale preparation and QC of phytase assay substrate from rice bran. *Anal Biochem*. 2019;**578**:7-12. doi:10.1016/j.ab.2019.04.021
13. Lu S, Shen Q, Zhang J. Allosteric Methods and Their Applications: Facilitating the Discovery of Allosteric Drugs and the Investigation of Allosteric Mechanisms. *Acc Chem Res*. 2019;**52**(2):492-500. doi:10.1021/acs.accounts.8b00570
14. Cooper WT HM, Salters VJ. . High-performance chromatographic separations of inositol phosphates and their detection by mass spectrometry. Inositol phosphates. Inositol phosphates: linking agriculture and the environment: *CABI*. 2007.p.23-40. doi:10.1079/9781845931520.0023
15. Sanikommu S, Pasupuleti M, Vadalkonda L. Comparison of phosphate estimating methods in the presence of phytic acid for the determination of phytase activity. *Prep Biochem Biotechnol*. 2014;**44**(3):231-241. doi:10.1080/10826068.2013.797434
16. Qvirist L, Carlsson N-G, Andlid T. Assessing phytase activity. *J Biological Method*. 2015;**2**(1). doi:10.14440/jbm.2015.58
17. Wyss M, Brugger R, Kronenberger A, Rémy R, Fimbel R, Oesterhelt G, *et al*. Biochemical characterization of fungal phytases (myo-inositol hexakisphosphate phosphohydrolases): catalytic properties. *Appl Environmen Microbiol*. 1999;**65**(2):367-373. doi:10.1128/aem.65.2.367-373.1999
18. YU XN, QIAN CX, SUN LZ. Chemosynthesis of nano-magnesium phosphates and its characterization. *Dig J Nanomater Biostructures*. 2016;**11**:1099-1103.
19. Yu X ZQ. Phosphate-Mineralization Microbe Repairs Heavy Metal Ions That Formed Nanomaterials in Soil and Water. *Nanomaterials-Toxicity, Human Health and Environment*. 2019. doi:10.5772/intechopen.84296
20. Hong R, Ting L, Huijie W. Optimization of extraction condition for phytic acid from peanut meal by response surface methodology. *Resource-Efficient Technologies*. 2017;**3**(3):226-231. doi:10.1016/j.reffit.2017.06.002
21. Rodriguez E, Han Y, Lei XG. Cloning, sequencing, and expression of an Escherichia coli acid phosphatase/phytase gene (appA2) isolated from pig colon. *Biochem Biophys Res Commun*. 1999;**257**(1):117-123. doi:10.1006/bbrc.1999.0361
22. Kim H-W, Kim Y-O, Lee J-H, Kim K-K, Kim Y-J. Isolation and characterization of a phytase with improved properties from Citrobacter braakii. *Biotechnol Lett*. 2003;**25**(15):1231-1234.
23. Melanie IS, Nicolas Le Novère. Cooperative binding. *PLoS Comput Biol*. 2013;**9**(6):e1003106. doi:10.1371/journal.pcbi.1003106
24. Gunasekaran K, Ma B, Nussinov R. Is allostery an intrinsic property of all dynamic proteins? *Proteins*. 2004;**57**(3):433-443. doi:10.1002/prot.20232
25. Sommerfeld V, Omotoso AO, Oster M, Reyer H, Camarinha-Silva A, Hasselmann M, *et al*. Phytate Degradation, Transcellular Mineral Transporters, and Mineral Utilization by Two Strains of Laying Hens as Affected by Dietary Phosphorus and Calcium. *Animals (Basel)*. 2020;**10**(10). doi:10.3390/ani10101736